Appendix

Nomenclature

Abbrevation	Definition
A-SVM	Adaptive Support Vector Machine
ANN	Artificial Neural Network
AUC	Area Under Curve
BCI	Brain-Computer-Interface
BB	Biceps Brachii
BP	Bereitschaftspotential
CNN	Convolutional Neural Network
CSP	Common Spatial Patterns
DBS	Deep Brain Stimulation
EEG	Electroencephalography
EMG	Electromyography
EMS	Electrical Muscle Stimulation
ERD	Event Related Desynchronisation
ERS	Event Related Synchronisation
FDS	Flexor Digitorium Superficialis
FOG	Freezing of Gait
FUS	Focused Ultrasound
FTtM	From Thought to Movement
GDPR	The General Data Protection Regulation
GPi	Globus Pallidus Internus
IMU	Inertial Measurement Unit
KNN	K-Nearest Neighbour
LSTM	Long Short-Term Memory
MCI	Mild Cognitive Impairment
MLP	Multi-Layer Perceptrons
ORICA	Online Recursive Independent Component Analysis
RNN	Recursive Neural Network
STN	Subthalamic Nucleus
SVM	Support Vector Machine
TB	Triceps Brachii
TBLH	Triceps Brachii Long Head
TKEO	Teager-Kaiser Energy Operator

References

[1]
L. Zhang *et al.*, 'Activation of Piezo1 by ultrasonic stimulation and its effect on the permeability of human umbilical vein endothelial cells', *Biomedicine & Pharmacotherapy*, vol. 131, p. 110796, Nov. 2020, doi: 10.1016/j.biopha.2020.110796.

[2]
D. Zhang, C. Hansen, F. D. Fréne, S. P. Kærgaard, and W. Qian, 'Automated labeling and online evaluation for self-paced movement detection BCI', *Knowledge-Based Systems*, vol. 265, p. 110383, Feb. 2023, doi: 10.1016/j.knosys.2023.110383.

[3]
R. A. Zanini, E. L. Colombin, and M. C. F. de Castro, 'Parkinson's disease EMG signal prediction using Neural Networks', *2019 IEEE International Conference on Systems, Man and Cybernetics (SMC)*, pp. 2446–2453, Sep. 2019.

[4]
H.-C. Wang, A. J. Lees, and P. Brown, 'Impairment of EEG desynchronisation before and during movement and its relation to bradykinesia in Parkinson's disease', *Journal of Neurology, Neurosurgery & Psychiatry*, vol. 66, no. 4, pp. 442–446, Apr. 1999, doi: 10.1136/jnnp.66.4.442.

[5]
A. A. P. Suárez, S. B. Batista, I. P. Ibáñez, E. C. Fernández, M. F. Campos, and L. M. Chacón, 'EEG-Derived Functional Connectivity Patterns Associated with Mild Cognitive Impairment in Parkinson's Disease', *Behavioral Sciences (Basel)*, vol. 11, no. 3, p. 11030040, Mar. 2021, doi: 10.3390/bs11030040.

[6]
V. del C. Silva-Acosta, I. Román-Godínez, S. Torres-Ramos, and R. A. Salido-Ruiz, 'Automatic estimation of continuous elbow flexion–extension movement based on electromyographic and electroencephalographic signals', *Biomedical Signal Processing and Control*, vol. 70, p. 102950, Sep. 2021, doi: 10.1016/j.bspc.2021.102950.

[7]
A. Saikia, A. Saikia, Amit Ranjan Barua, and S. Paul, 'EEG-EMG Correlation for Parkinson's disease', *International Journal of Engineering and Advanced Technology (IJEAT)*, vol. 8, no. 6, Aug. 2019, doi: 10.35940/ijeat.F8360.088619.

[8]
A. Miladinović *et al.*, 'EEG changes and motor deficits in Parkinson's disease patients: Correlation of motor scales and EEG power bands', *Procedia Computer Science*, vol. 192, pp. 2616–2623, 2021, doi: 10.1016/j.procs.2021.09.031.

[9]
M. Mahmoodi, Bahador Makkiabadi, M. Mahmoudi, and S. Sanei, 'A new method for accurate detection of movement intention from single channel EEG for online BCI', *Computer Methods and Programs in Biomedicine Update*, vol. 1, p. 100027, Aug. 2021, doi: 10.1016/j.cmpbup.2021.100027.

[10]
C. R. Oehrn *et al.*, 'Chronic adaptive deep brain stimulation versus conventional stimulation in Parkinson's disease: a blinded randomized feasibility trial', *Nature Medicine*, vol. 30, pp. 3345–3356, Aug. 2019, doi: doi.org/10.1038/s41591-024-03196-z.

[11]
D. Liao, F. Li, D. Lu, and P. Zhong, 'Activation of Piezo1 Mechanosensitive Ion Channel In HEK293T Cells by 30 MHz Vertically Deployed Surface Acoustic Waves', *Biochemical and Biophysical Research Communications*, vol. 518, no. 3, pp. 541–547, Oct. 2019, doi: 10.1016/j.bbrc.2019.08.078.

[12]
N. Kueper *et al.*, 'EEG and EMG dataset for the detection of errors introduced by an active orthosis device', *Frontiers in Human Neuroscience*, vol. 18, p. 1304311, Jan. 2024, doi: 10.3389/fnhum.2024.1304311.

[13]

F. Karimi, J. Niu, K. Gouweleeuw, Q. Almeida, and N. Jiang, 'Movement-related EEG signatures associated with freezing of gait in Parkinson's disease: an integrative analysis', *Brain Communications*, vol. 3, no. 4, p. fcab277, Nov. 2021, doi: 10.1093/braincomms/fcab277.

[14]

S. Farashi, A. Sarihi, M. Ramezani, S. Shahidi, and M. Mazdeh, 'Parkinson's disease tremor prediction using EEG data analysis-A preliminary and feasibility study', *BMC Neurology*, vol. 23, p. 420, Nov. 2023, doi: 10.1186/s12883-023-03468-0.

[15]

K. Desai, 'Parkinson's Disease Detection via Resting-State Electroencephalography Using Signal Processing and Machine Learning Techniques', *arxiv*, Mar. 2023, doi: 10.48550/arXiv.2304.01214.

[16]

M. Conti *et al.*, 'Brain Functional Connectivity in de novo Parkinson's Disease Patients Based on Clinical EEG', *Frontiers in Neurology*, vol. 13, p. 844745, Mar. 2022, doi: 10.3389/fneur.2022.844745.

[17]

A. Buerkle, W. Eaton, N. Lohse, T. Bamber, and P. Ferreira, 'EEG based arm movement intention recognition towards enhanced safety in symbiotic Human-Robot Collaboration', *Robotics and Computer-Integrated Manufacturing*, vol. 70, p. 102137, Aug. 2021, doi: 10.1016/j.rcim.2021.102137.

[18]

M. J. Antony *et al.*, 'Classification of EEG Using Adaptive SVM Classifier with CSP and Online Recursive Independent Component Analysis', *Sensors (Basel)*, vol. 22, no. 19, p. 7596, Oct. 2022, doi: 10.3390/s22197596.

[19]

J. Aeles, F. Horst, S. Lapuschkin, L. Lacourpaille, and F. Hug, 'Revealing the unique features of each individual's muscle activation signatures', *The Royal Society Publishing Interface*, vol. 18, no. 174, p. 20200770, Jan. 2021, doi: 10.1098/rsif.2020.0770.

Figures and tables

AI-model	Precision	Training time (s)	Time (hh:mm:ss)	AUC	Efficiency	Parameters
A-SVM	85.67%	57	00.00.57	93.36%	79.81%	N/A
CNN	100.00%	1329	00.22.09	100.00%	83.88%	907554
DeepConvNet	99.87%	1063	00.17.43	100.00%	84.86%	1073474
LSTM-CNN	99.92%	3655	01.00.55	100.00%	78.72%	842146
LSTM-RNN	97.58%	14165.18	03.56.05	99.33%	69.54%	548642
SVM	67.29%	8	00.00.08	69.48%	58.44%	N/A
Transformer	98.50%	645	00.10.45	99.97%	85.77%	505410

Figure 1: First iteration of AI-model training, using K-fold cross-validation and different amount of parameters[1]. The models might have overfitted in this iteration, because of the high precisions achieved. The models were built to classify between non-movement and movement in EEG and EMG signals.[2]

---

[1] Unlike neural networks, SVMs do not learn internal parameters through backpropagation but rely on support vectors and kernel functions, resulting in fewer tuneable parameters
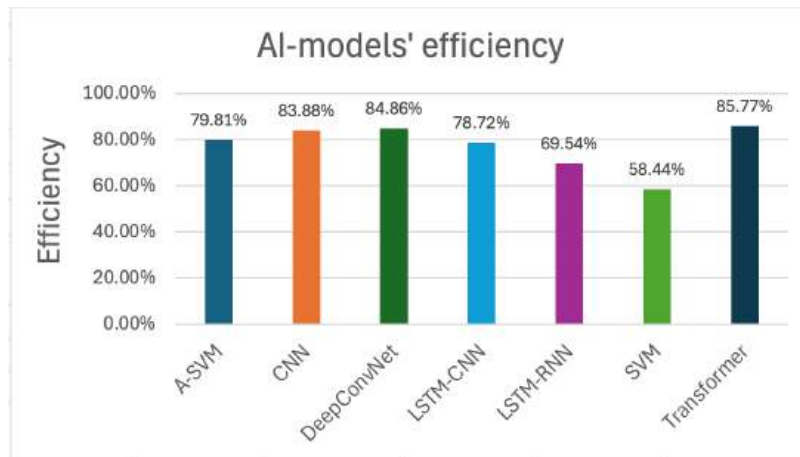
[2] Own work in Excel

Figure 2: Graph of AI-models' efficiency[3]

AI-model	Precision	Training time / s	Inference time / s	Time (hh:mm:ss)	AUC	Efficiency	Parameters	F1-score
A-SVM	64.91%	9.89	0.0016	00.00.09	94.04%	58.62%	N/A	73.89%
CNN	96.99%	142.05	0.000712	00.02.22	94.17%	68.56%	229876	90.37%
DeepConvNet	98.25%	103.50	0.00061	00.01.43	96.51%	73.32%	269218	92.68%
LSTM-CNN	92.86%	320.18	0.001545	00.05.20	91.07%	56.99%	191090	86.01%
LSTM-RNN	92.11%	2245.71	0.09465	00.37.25	94.58%	40.33%	243234	89.93%
SVM	50.12%	1.19	0.000051	00.00.01	59.57%	43.66%	N/A	66.78%
Transformer	88.47%	3615	0.018	01.00.15	94.28%	34.37%	227234	83.03%

Figure 3: Second iteration of AI-model training, using GroupKFold cross-validation and around the same amount of parameters to better compare different architectures. The precisions have decreased and the models likely did not overfit this time. The models were built to clasify between non-movement and movement in EEG and EMG signals.[4]
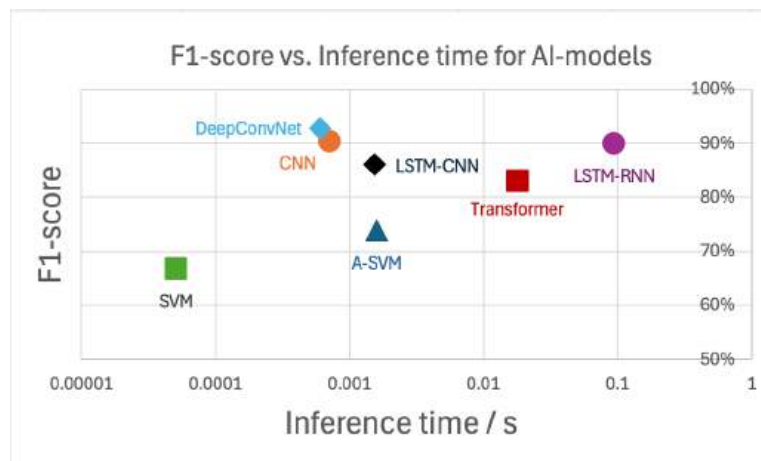

Figure 4: Graph of AI-models' F1-score vs. Inference time. The x-axis is in a logarithmic scale of 10. Even though the Transformer performed worse here, I have worked extensively with this model type before, which allows me to keep developing and improving it, especially because it fits well with combining EEG, EMG, and IMU signals in real-time. Its performance is also likely to improve with more training data and better hyperparameter tuning[5].

---

[3] Own work in Excel
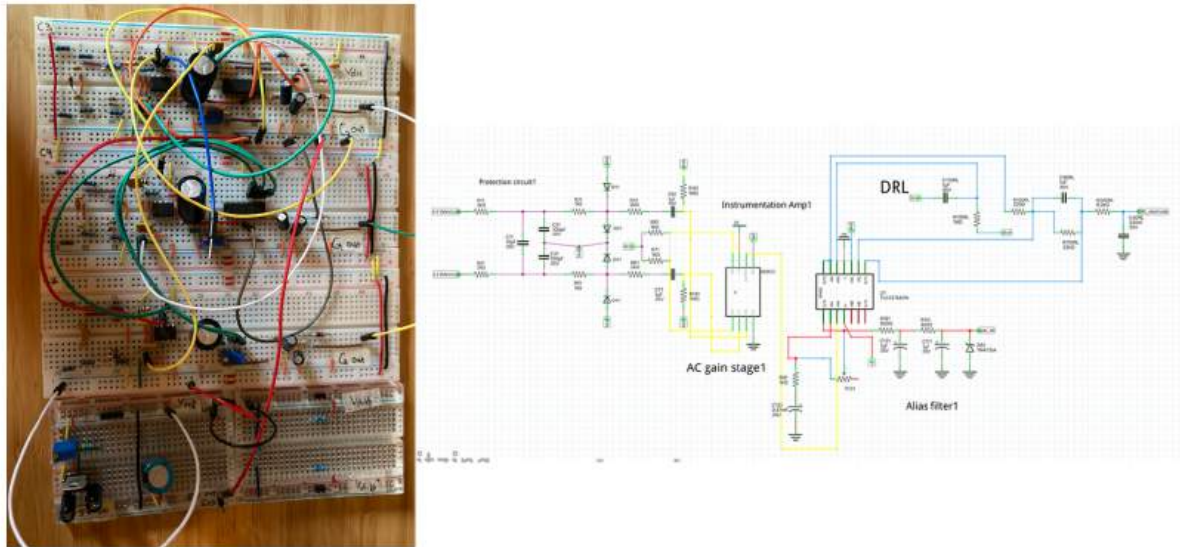[4] Own work in Excel
[5] Own work in Excel

Figure 5: On the left is the homebuilt EEG-circuit used for the project, it consists of a protection stage, an instrumentation amplifier (AD623), an AC gain stage, a low-pass anti-aliasing filter, and a shared Driven Right Leg (DRL) feedback unit for common-mode noise reduction. On the right is the circuit diagram shown. This structure is identically replicated for a total of three active electrodes (C3, C4, and Cz), making the final system a triplicated version of the circuit shown here[6].

Figure 6: Electrode placement with EEG-hardware donated by OpenBCI[7]
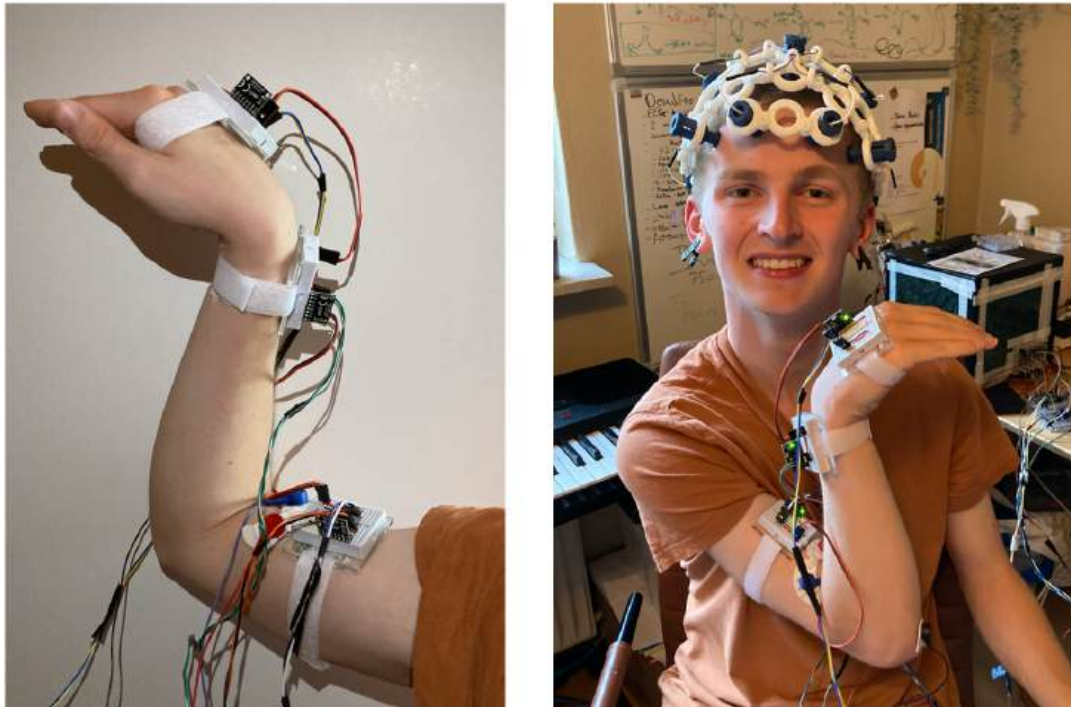
---

[6] Own work in Fritzing
[7] Own work

Figure 7: Three IMUs are mounted on the right arm to track motion dynamics. Surface EMG is recorded from the BB using an active electrode, with a nearby reference electrode and ground placed at the elbow. EEG signals are acquired using the OpenBCI Cyton board and 8-channel EEG headset (donated by OpenBCI)[8]
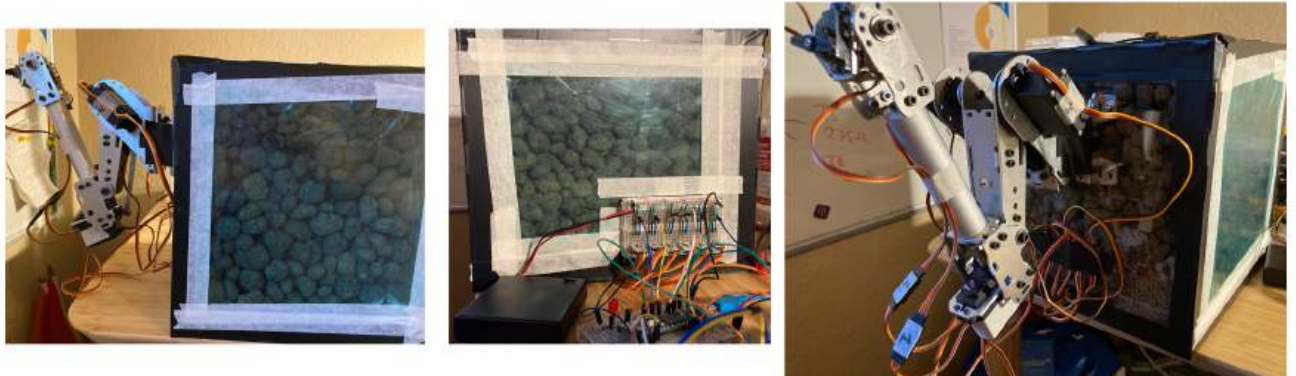

Figure 8: Homebuilt 6-axis robotic arm. The robotic arm is mounted on a custom box designed to mimic human arm anatomy. Servo cables pass through the box and connect to a Teensy 4.1 microcontroller, which receives real-time input from EEG, EMG, and IMU devices. This integration enables real-time biosignal-driven control of the arm[9].
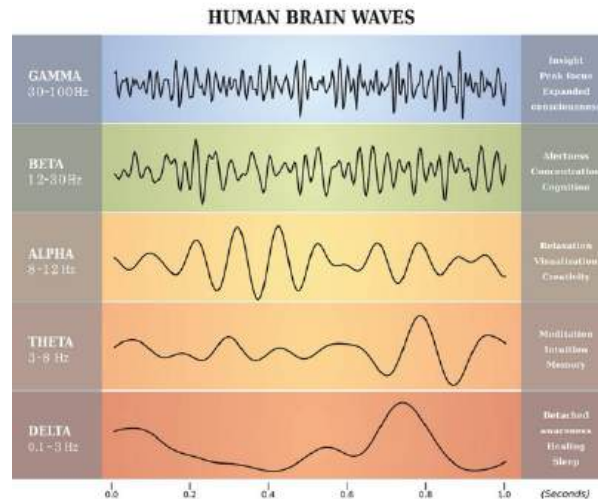
---

[8] Own work
[9] Own work

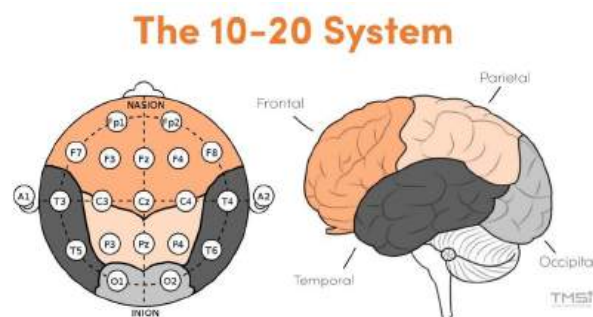*Figure 9: An overview of the different frequency bands and the different mental states associated with them[10]*

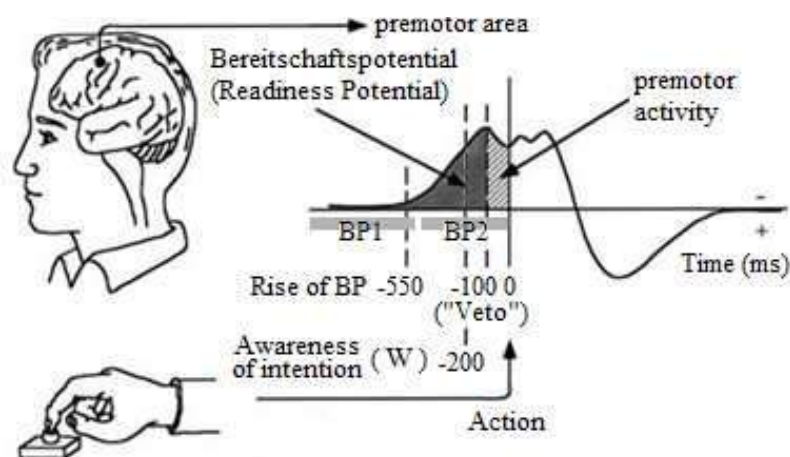*Figure 10: The international 10/20 system for the placement of EEG-electrodes[11]*

Figure 11: An example of a BP.[12]

[10] Loaned from https://coronatodays.com/5-types-of-brain-waves-and-their-link-to-different-states-of-consciousness/
[11] Loaned from https://info.tmsi.com/blog/the-10-20-system-for-eeg
[12] Loaned fromf https://www.researchgate.net/figure/Bereitschaftspotential-and-the-Libets-experiment-At-550-ms-the-rise-of-BP-at-200-ms_fig14_268216375

Category	Goal	Technology	Degree of invasiveness	The patient	Application of AI	Training
BCI	Communication and control by using brain signals	EEG or implants	Non-invasive (EEG) or invasive (implants)	Neurological disorders	Limited	Comprehensive signal training
Neuroprost hetics	Rehabilitation of motoric functions	EMG/EEG + actuator	Often invasive	Loss of motoric function	Limited	Calibration on muscle activity
DBS	Symptom treatment by brain stimulation	Implanted electrodes and a pulse generator	Very invasive	Parkinson's-disease and tremor	None	Not needed
FTtM	Prediction and active assistance of movement by intention	Wearable EEG with a Transformer-model	Non-invasive	Parkinson's-disease and other mobility disorders	Transformer-model trained on multimodal data	Training on the user's own data

Figure 12: A comparison between this project and similar solutions. FTtM stands out as a non-invasive, wearable, and adaptive neurotechnology that integrates the body's own biosignals. [13]

Movement	No movement (baseline)	Flexion of underarm	Extension of underarm	Raising of arm	Lowering of arm	Supination of wrist	Pronation of wrist
Photo of Movement							
Binary value	0000	0001	0010	0011	0100	0101	0110

Figure 13: The different arm movements and their correspondring binary values[14]

Nr.	Functional Requirement
F1	The system must acquire EEG, EMG, and IMU data with high signal quality and effective noise filtration.
F2	The transformer model must predict intentional muscle movements based solely on real-time EEG data.
F3	Electrodes and sensors must be safely and comfortably mounted on the user's head and arm, without causing irritation.
F4	The system must be able to initiate and assist movement using neural intentions alone.
F5	The system must operate in real time: binary movement classification should occur within milliseconds of the user's intention.
F6	The system must be wearable and include a compact transformer model with an integrated battery.
F7	The system must be medically neutral and must not interfere with medications such as Levodopa.
F8	The system must translate the Transformer model's output into physical movement via an actuator (EMS/FUS).
F9	The system must prevent unintended movements. A stop function, either analog or digital, must deactivate the system immediately.
F10	The system must operate continuously for at least 16 hours, allowing overnight recharging for full-day use.

Nr.	Non-functional Requirement
NF1	The final system must be economically accessible and cost-efficient.
NF2	The system must be individualised, supporting person-specific training due to variations in EEG signals and brain structures.
NF3	The system must be scalable: transitioning from personalised models to adaptive models generalisable across different users.
NF4	The user interface (GUI) must be intuitive and user-friendly, allowing easy access for both patients and clinical staff.
NF5	The system must be robust for daily use, including resistance to movement, moisture, humidity, and minor impacts.
NF6	The system must be adjustable to accommodate different body sizes and types of motor impairments.
NF7	The transformer model must provide explainability, e.g., by logging its predictions to a database for post-hoc error analysis.
NF8	User signal data must be processed confidentially and never stored or shared without explicit informed consent.

Figure 14: Functional and Non-functional requirements for the system[15]

---

[13] Own work
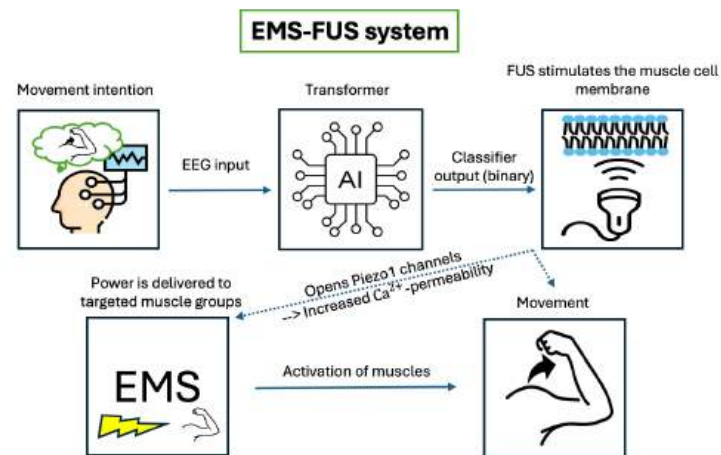[14] Own work in Word
[15] Own work in Word

Figure 15: A visualisation of the EMS-FUS system proposed in this project to enable voluntary movements through neural signals[16].
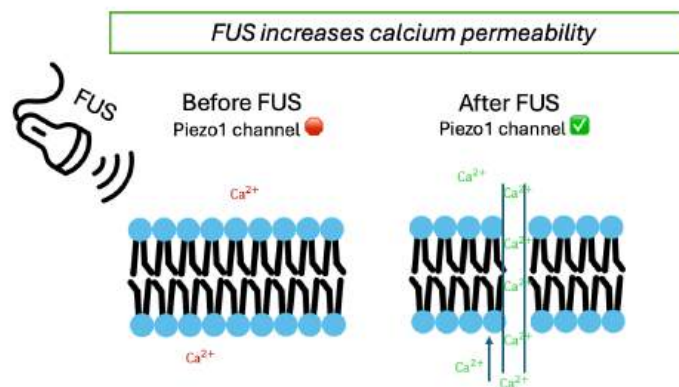

Figure 16: How FUS increases calcium permeability in the Piezo1 channel[17]

[16] Own work in PowerPoint
[17] Own work in PowerPoint

Article	Datatype	AI-model	Precision/Results	Main conclusion
Antony et al., 2022	EEG	A-SVM	91%	Feature extraction improves the precision
Buerkle et al., 2021	EEG	LSTM-RNN	84-82% (real-time)	AI-models can be used to real-time detection of movement
Zhang et al., 2023	EMG	DeepConvNet	100%	Movement can precisely be detected in EMG
Aeles et al., 2021	EMG	SVM	99.3%	EMG-signals are individual
Silva-Acosta et al., 2021	EEG + EMG	LSTM	Precision increased when gender was separated s	EEG combined with EMG improves the precision
Mahmoodi et al., 2021	EEG (BP) + EMG	TKEO (threshold)	91.2% (real-time)	It is possible to detect movement intention
Karimi et al., 2021	EEG + EMG	-	⬇Beta, ⬆Theta	EEG-patterns are changed in Parkinson's patients
Wang et al., 1999	EEG	-	Levodopa reduces Parkinson's symptoms	Dopamine excitable medicine is a treatment against Parkinson's disease
Miladinovic et al., 2021	EEG	-	⬇Aloha, Beta, ⬇Delta, Theta	EEG-patterns changes during worsen of Parkinson's disease
Farashi et al., 2023	EEG + IMU	KNN	81.3%	EEG can predict when tremor initiates
Peláez Suárez et al., 2021	EEG	-	⬇Alpha, Delta (connectivity)	EEG-patterns are changed in MCI Parkinson's patients
Conti et al., 2022	EEG	-	⬇Alpha, Beta	De novo Parkinson's patients had lower Alpha- and Beta connectivity
Desai, 2023	EEG	Random Forest	97.5%	It is possible to distinguish between healthy subjects and Parkinson's patients via EEG-signals
Zanini et al., 2019	EMG	MLP/LSTM	High precision	AI can predict EMG for electrical stimulation
Saiki et al., 2019	EEG + EMG	ANN	98.8%	Multimodal > single data type

Figure 17: This table summarises selected studies based on their data type, AI model, performance, and main conclusions. The colour coding indicates the focus of each article: grey = EEG-specific studies, yellow = EMG-specific studies, green = studies combining EEG and EMG, and blue = Parkinson's disease-specific studies involving multiple modalities (EEG, EMG, and IMU)[18].

Nr.	Place	Substrate	Product	Enzyme	Cofactor	Reaction type	Comment
1	The gut	L-DOPA	(the same)	LAT1	-	Facilitated transport	No chemical reaction
2	The blood (periphery)	L-DOPA	Dopamine	AADC	PLP	Decarboxylation	AADC inhibited by carbidopa
3	The blood (periphery)	L-DOPA	3-O-methyldopa	COMT	SAM → SAH	O-methylering	Inactive metabolite
4	BBB	L-DOPA	(the same)	LAT1	-	Facilitated transport	Transported over BBB - dopamine is not able to
5	The brain	L-DOPA	Dopamine	AADC	PLP	Decarboxylation	In dopaminerge neurons
6	The brain	Dopamine	3-methoxytyramin	COMT	SAM → SAH	O-methylering	Inhibited by central COMT-inhibitors (tolcapon)
7a	The brain	Dopamine	DOPAL	MAO-B	FAD	Oxidativ deamination	MAO-B removes amino group
7b	The brain	DOPAL	DOPAC	ALDH	NAD+	Aldehyde-oxidation	Detoxification of DOPAL, produces carboxyl acid
8	The brain	DOPAC	Homovanillin acid	COMT	SAM → SAH	O-methylering	Last step in the dopamine metabolism before excretion in the urine
9a	The brain	3-methoxytyramin	Methoxy-DOPAL	MAO-B	FAD	Oxidativ deamination	MAO-B removes amino group, produces aldehyde
9b	The brain	Methoxy-DOPAL	Homovanillin acid	ALDH	NAD+	Aldehyde-oxidation	Detoxification, aldehyde oxidates to carboxyl acid

Figure 18: This table outlines the absorption, transport, enzymatic conversion, and breakdown of L-DOPA and its derivatives, highlighting locations, enzymes, cofactors, and clinical relevance. It contextualizes the neurochemical foundation for treating Parkinson's disease and supports the project's aim to remain pharmacologically neutral[19].

---

[18] Own work
[19] Own work